



# Phase distribution, migration and relationship of polychlorinated dibenzo-p-dioxins and dibenzofurans and heavy metals in a large-scale hazardous waste incinerator

Shijian Xiong, Yaqi Peng<sup>\*\*</sup>, Ken Chen, Shengyong Lu<sup>\*</sup>, Wenqian Jiang, Xiaodong Li, Fei Wang, Kefa Cen

State Key Laboratory of Clean Energy Utilization, Zhejiang University, Hangzhou, 310027, PR China

## ARTICLE INFO

Handling editor: Zhen Leng

### Keywords:

Polychlorinated dibenzo-p-dioxins and dibenzofurans  
Heavy metals  
Hazardous waste incineration  
Phase distribution  
Relationship

## ABSTRACT

Polychlorinated dibenzo-p-dioxins and dibenzofurans (PCDD/F) and heavy metals emitted from hazardous waste incinerators have aroused public concern due to the risks to the environment and human health. In the study, phase distribution, migration, and relationship of PCDD/F and heavy metals (arsenic, cadmium, chromium, copper, mercury, nickel, plumbum, zinc) are investigated in a typical hazardous waste incinerator. The PCDD/F mass concentrations and toxic equivalent quantity are reduced to 3.26 ng/Nm<sup>3</sup> and 0.0484 ng/Nm<sup>3</sup> by air control pollution devices, with 93.1% remove efficiency. High sulfur content in hazardous waste results in low PCDD/F and heavy metals emissions. Moreover, migration analysis of PCDD/F mass concentrations indicates that vast PCDD/F migrates to the mixtures with sodium bicarbonate and activated carbon (52.4%), followed by fly ash (21.8%), sodium hydroxide solution (19.3%), and atmosphere (6.49%). Furthermore, TCDF isomers (37%) dominate among the PCDD/F congeners, while 1,2,3,4,6,7,8-HpCDF (20%) dominates among 2,3,7,8-substituted congeners. Deduced by the ratio of PCDF/PCDD, the dominant mechanism of PCDD/F is de novo synthesis and chlorobenzene route synthesis. Based on the relative enrichment index, heavy metals are classified into three types: volatile heavy metals (plumbum, zinc, cadmium, mercury), medium volatile heavy metals (copper, chromium, arsenic), involatile heavy metals (nickel). Additionally, copper is inclined to deposit into the bottom slag as CuSO<sub>4</sub> rather than the volatile substance due to high levels of sulfur dioxide (3000 parts per million). The migration behavior of heavy metals is dependent on the volatility properties of these metals. Statistically, PCDD/F emissions have the highest correlation coefficient with plumbum ( $r = 0.815$ ), followed by nickel ( $r = -0.798$ ). Besides, the PCDD/F formation is promoted by the volatile heavy metal, prevented by medium volatile heavy metals. The study not only provides a comprehensive understanding of PCDD/F and heavy metals characteristics but also effective and feasible strategies to reduce the toxic pollutants emissions in large-scale hazardous waste incinerators.

## 1. Introduction

Rapid industrialization has resulted in an increasing quantity of industrial hazardous waste, especially in developing countries, like China. On the basis of the newest statistics in China, the quantity of hazardous waste (HW) increased from 15.89 in 2010 to 65.91 million tons in 2017 (National Bureau of Statistics of China). Although there is no accurate amount of hazardous in 2020, the quantity of HW can be estimated to be 100 million tons, considering the growth rate and the effect of

COVID-19. Hence, a large amount of HW, including industrial hazardous waste and medical waste, contains heavy metals and toxic organic pollutants, resulting in potential risks to the environment. At present, incineration has been considered as a preferred technology to dispose of HW in China because of the advantages including chemical-toxicity destruction, outstanding volume reduction, and energy recovery.

However, the incineration for HW disposal presents a disadvantage in which secondary pollutants are emitted, especially toxic pollutants. The toxic pollutants from hazardous waste incinerators (HWI) include heavy metals and persistent organic pollutants, especially

\* Corresponding author.

\*\* Corresponding author.

E-mail addresses: [pengyaqi@zju.edu.cn](mailto:pengyaqi@zju.edu.cn) (Y. Peng), [lushy@zju.edu.cn](mailto:lushy@zju.edu.cn) (S. Lu).

<https://doi.org/10.1016/j.jclepro.2022.130764>

Received 12 September 2021; Received in revised form 9 January 2022; Accepted 29 January 2022

Available online 1 February 2022

0959-6526/© 2022 Elsevier Ltd. All rights reserved.

Nomenclature			
AC	activated carbon	HxCDF	hexachlorodibenzo-p-furan
ACI	activated carbon injection	HWI	hazardous waste incinerator
APCD	air pollution control devices	HW	hazardous waste
$C_{in}$	pollutants concentrations ( $\text{ng}/\text{Nm}^3$ ) at the inlet of every unit	I-TEQ	international toxic equivalents
$C_{out}$	pollutants concentrations ( $\text{ng}/\text{Nm}^3$ ) of the same items at the outlet of each unit	$n_i$	number of hydrogen atoms substituted by chlorine
$C_{total}$	concentrations ( $\text{ng}/\text{Nm}^3$ ) at the outlet of the quench tower	OCDD	octachlorodibenzodioxin
$C_{SO_2}$	$\text{SO}_2$ concentrations ( $\text{mg}/\text{Nm}^3$ )	OCDF	octachlorodibenzofuran
$d_c$	degree of chlorination	PCDD	polychlorinated dibenzo-p-dioxin
DS	dry scrubber	PCDF	polychlorinated dibenzo-p-furan
EPA	environment protect agency	PCDD/F	polychlorinated dibenzo-p-dioxins and -furans
f	weight percentage (%) of PCDD, PCDF, or PCDD/F congeners	PeCDD	pentachlorodibenzo-p-dioxin
FF	fabric filter	PeCDF	pentachlorodibenzo-p-furan
HpCDD	heptachlorodibenzo-p-dioxin	MR	migration rate (%)
HpCDF	heptachlorodibenzo-p-furan	$MR_{AC\&NaHCO_3}$	migration rate (%) of PCDD/F to AC&NaHCO <sub>3</sub>
HxCDD	hexachlorodibenzo-p-dioxin	$MR_{AC}$	migration rate (%) of PCDD/F to AC
		$MR_{NaOH}$	migration rate (%) of PCDD/F to NaOH solution
		REI	relative enrichment indexes
		TCDD	tetrachlorodibenzo-p-dioxin
		TCDF	tetrachlorodibenzo-p-furan
		WS	wet scrubber

polychlorinated dibenzo-p-dioxins and dibenzofurans (PCDD/F). Due to mobility, fatality, bioaccumulation of heavy metals (Chang et al., 2000; Margallo et al., 2015), and the high toxicity, potentially carcinogenic and mutagenic effects of PCDD/F, potential risks are exposed to humans and the environment. Therefore, it is far important to control emissions to the legislation limit for the industrial managers, government, and researchers. The PCDD/F emissions were characterized in a HWI under a series of operating conditions and HW compositions (Gullett et al., 2000). Moreover, the PCDD/F emission levels were compared under start-up, shut-down, and normal operating conditions (Li et al., 2017). Besides, the influence of active carbon injection (ACI) coupled with fabric filter (FF) or wet scrubber (WS) on PCDD/F emissions was also investigated in a HWI (Cao et al., 2018). In addition, emission reduction strategies were conducted by adding chlorobenzenes or chlorophenols to raw material (Wang et al., 2019). These researches mainly focused on PCDD/F emission levels on a single unit.

Generally speaking, the PCDD/F formation mechanism in thermal processes is divided into three types based on previous researches: (1) homogeneous gas-phase reaction (500–800 °C) (Louw and Ahonkhai, 2002) in which molecular/radical or radical/radical couples to form PCDD/F; (2) heterogeneous precursor reaction (200–500 °C) (Altwicker, 1996) in which chlorophenols or chlorobenzenes are catalyzed; (3) de novo synthesis (Altwicker, 1996; Huang and Buekens, 1996) in which PCDD/F are formed from polycyclic aromatic hydrocarbons and carbon matrix on fly ash or soot from 200 °C to 500 °C. Based on the comprehensive research (Huang and Buekens, 1996; Nganai et al., 2014; Xiong et al., 2021), if the total concentrations of PCDF are higher than that of PCDD, the PCDD/F formation will be dominated by de novo synthesis and the chlorobenzene route synthesis. At present, there is still controversy over the dominant mechanism of the PCDD/F formation in HWI, subject to 17 toxic congeners rather than 136 congeners. Besides, the PCDD/F formation was proven to be inhibited by adding inhibitors containing sulfur or nitrogen, or phosphorus (Ke et al., 2010; Ruokojärvi et al., 2001; Ryan et al., 2006), due to the metal catalyst (CuCl<sub>2</sub> et al.) poisoned and chlorination reaction hindered. However, it is uncertain that the HW with high levels of sulfur content has an inhibition effect when the concentrations of heavy metals are also high levels during HWI.

To control the pollutants from HWI, air pollution control devices (APCD) are used at the end of the rotary kiln, including quench tower, dry scrubber (DS), ACI coupled FF, and WS. The ACI coupled FF, and WS have been proven to influence the PCDD/F characteristics (Chen et al.,

2020). The quench tower is designed to reduce the PCDD/F formation in the temperature range from 500 to 200 °C by cooling the flue gas quickly. Theoretically, the de novo synthesis can be suppressed by the method. The suppression effect of the quench tower has been investigated, suggesting that the quench tower succeeds to reduce the PCDD/F emissions (Wang et al., 2019), excluding the condition where the raw materials contain high content of chlorobenzenes. The memory effect can be caused by wet scrubbers (Lothgren and van Bavel, 2005), resulting in degrading the removal of PCDD/F. The dry scrubber is mainly used to control the HCl thereby inhibiting deacon reaction, which can promote the formation of PCDD/F. However, few evaluations to investigate the effect of the DS have been reported. In fact, rare systematic research has been reported about the PCDD/F and heavy metal along with the APCD in HWI. Therefore, the migration and phase distribution of PCDD/F along APCD are vague. It is crucial for the optimization of APCD operation, exposure risks understanding, and pollutants emission control.

In the post-combustion zone, a high level of heavy metals was emitted from HWI and undergo the process of evaporation, condensation, particle collection in APCD (Li et al., 2018). The distribution characteristics of heavy metals from HWI can provide guidance on the design of APCD and an accurate control strategy to abate certain types of heavy metals. Previous studies have adopted the typical procedure to study the distribution characteristics by comparing the concentrations in a series of samples of solid residue or flue gas. Heavy metals have been proven to be captured with ligand-based composite materials (Alam et al., 2019a; Alam et al., 2019b; Awual, 2015, 2017, 2019a, b, c; Awual and Hasan, 2019; Awual et al., 2019; Islam, M.A. et al., 2019b; Kamel et al., 2019; Kubra et al., 2021; Rahman et al., 2019; Sheikh et al., 2017; Sheikh et al., 2018). The fly ash is mainly composed of silicon dioxide, calcium oxide, and aluminum oxide, which is with high porosity and a large specific surface area. Therefore, fly ash has been considered a sorbent to absorb heavy metals (Evans and Williams, 2000). Due to many significant elements to influence the distribution and migration of heavy metals (components of HW, operational parameters, type of APCD) (Belevi and Moench, 2000; Zhao et al., 2015), the distribution characteristics of heavy metals varied in different studies (Li et al., 2018; Wang et al., 2020). Furthermore, there is a rare study to explore the impact of high levels of heavy metals on PCDD/F formation, resulting in the lacking effective control.

In this study, the levels of PCDD/F and heavy metals are investigated in HWI along with APCD comprehensively. APCD includes the quench

tower, DS, ACI coupled with the FF, and WS. The objectives are: (1) to investigate the migration and phase distribution of PCDD/F along with the APCD in HWI; (2) to explore the impact of high levels of heavy metals on the PCDD/F formation by statistical methods; (3) to elucidate the dominant PCDD/F formation mechanism by 136 congeners signatures. Ultimately, the study aims to reveal phase distribution, migration, and relationship of PCDD/F, and heavy metals in a typical large-scale HWI. The study provides a comprehensive understanding of potential exposure risks from HWI and practical strategies to control PCDD/F and heavy metal emissions in a large-scale HWI.

## 2. Materials and method

### 2.1. Operating parameters of the incinerator and characteristics of hazardous waste

The full-scale HW incinerator is located in Shandong Province, China. Fig. 1 shows the schematic diagram, flue/stack gas sampling point, and ash sampling point. Before being fed into the rotary kiln, the HW was well broken and blended. The operating parameters of the HW incinerator are shown in Table 1. And the average feeding rate of HW is 89.8 t/d. A series of heat exchanger boilers are set to cool the flue gas from 1100 °C to 400 °C. The HW incinerator was operated based on the legal technical regulation to ensure the complete combustion of organic matter. Specifically, the temperature of the second combustion chamber was maintained above 1100 °C and longer than 2 s. And the excess air coefficient is more than 1.5 to maintain abundant oxygen.

APCD includes a quench tower, a DS, an ACI coupled with the FF, and a WS tower, aiming to remove pollutants. The active carbon (AC) power was injected between the quench tower and FF, with NaHCO<sub>3</sub> injected simultaneously. The injection rates of NaHCO<sub>3</sub> and AC were 62.5 and 96 kg/h, respectively. The WS with sodium hydroxide solution injection was set to remove acidic pollutants (HCl and SO<sub>2</sub>) and particulate matter. The large-scale incinerator and APCD have been considered as the mainstream for industrial managers due to the rapid increase of hazardous waste production in China. Hence, the study can be considered as typical work for the development of HWI. Prior to the comprehensive study, the bottom slag and fly ash adhered to the surface were removed to clean APCD and incinerator thoroughly, aiming to reduce

**Table 1**

Operating parameters of the HW incinerator and characteristics of hazardous waste.

Operating parameters	
Annual capacity (t·d <sup>-1</sup> )	100
Production of fly ash (t·h <sup>-1</sup> )	5.86
Production of bottom slag (t·h <sup>-1</sup> )	18.99
Volume fate of flue gas (Nm <sup>3</sup> ·h <sup>-1</sup> )	20650
Gas residence time (s)	3
Temperature of middle kiln (°C)	900
Temperature of second furnace outlet (°C)	1100
Temperature of boiler outlet (°C)	400
Temperature of quench tower outlet (°C)	190–200
Temperature of bag filter outlet (°C)	170–190
O <sub>2</sub> (%)	8.4
NO <sub>x</sub> (mg·Nm <sup>-3</sup> )	81.1
SO <sub>2</sub> (mg·Nm <sup>-3</sup> )	19.2
HCl (mg·Nm <sup>-3</sup> )	1.64
Characteristics of hazardous waste	
Moisture (wt%)	17.66
Ash (wt%)	36.14
Volatile matter (wt %)	42.23
Fixed carbon (wt %)	3.97
C (wt %)	29.99
H (wt %)	1.76
N (wt %)	2.43
S (wt %)	2.82
Cl (wt %)	5.26
O (wt %)	15.44

any potential influence on the experimental results. The raw hazardous waste was a homogenous mixture of phenolic waste and woodchips. The details of HW content were shown in Table 1.

### 2.2. Sampling and analysis methods

To study the migration of PCDD/F, PCDD/F samples were collected at A, B, C, D sampling points along with APCD. To collect PCDD/F samples in the flue/stack gas, an isokinetic sampler (Model KNJ23, KNJ, Korea) was used following EPA Method 23a. To observe the detailed phase distribution and evolution of PCDD/F, the gas phase and solid phase of PCDD/F were separated. Then, the samples were purified after a series of pretreatment, including soxhlet extraction and purification.

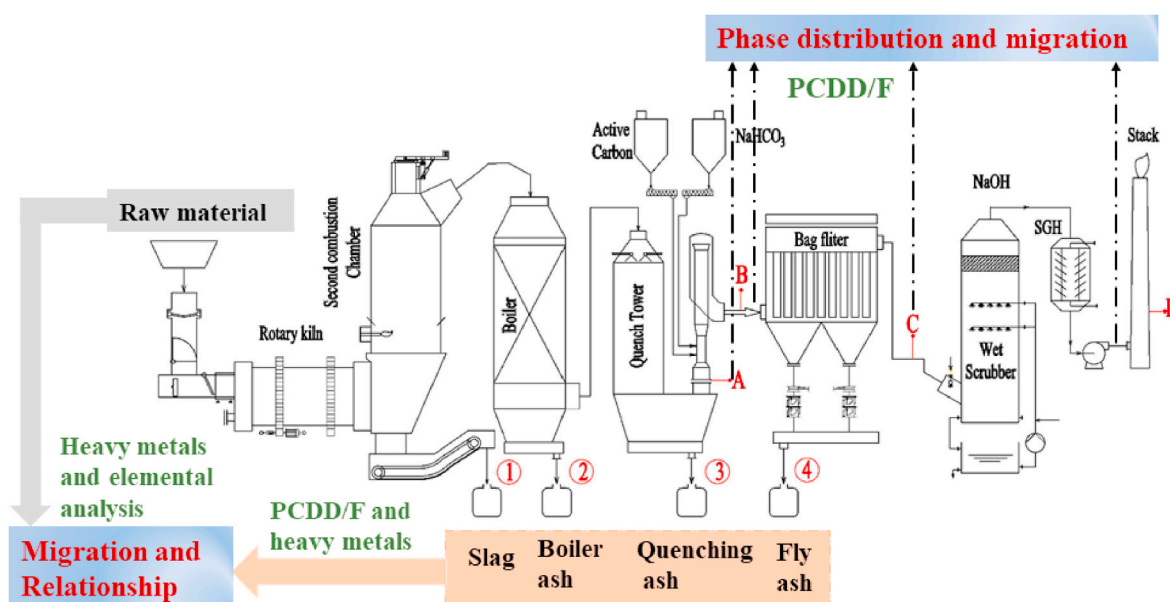


**Fig. 1.** The schematic diagram of the HWI (Four sampling points for the flue gas were: (A) the outlet of the quench tower; (B) the outlet of the DS; (C) the inlet of the WS; (D) the stack); (Four ash sampling points were: 1: the bottom of the second combustion; 2: the bottom of the boiler; 3: the bottom of quench tower; 4: the bottom of fabric filter).

The complete PCDD/F method was described in previous studies (Yan et al., 2006). The recoveries ranged from 50% to 130%, consistent with EPA Method 23. I-TEQ was computed according to NATO/CCMS factors (Bhavsar et al., 2008). Besides, the PCDD/F concentrations were converted to the standard condition where O<sub>2</sub> content was 11% with respect to temperature and pressure of 0 °C and 101.3 kPa. Furthermore, to study the relationship between PCDD/F and heavy metals in the residue, the PCDD/F samples from ①, ②, ③, ④ were determined by the EPA 1613 method, which was described in detail in the previous study (Chen et al., 2017). The SO<sub>2</sub> concentrations (C<sub>SO2</sub>) were measured simultaneously at sampling points C and D by a flue gas analyzer (MRU VARIO PLUS). The C<sub>SO2</sub> values were also normalized to the standard condition where O<sub>2</sub> content was 11% with respect to temperature and pressure of 0 °C and 101.3 kPa, respectively. This study focuses on the phase distribution and migration of PCDD/F in gas- and solid-phase during the APCD. The sampling for PCDD/F was carried out under the steady condition and sustained for 2h (4h for each sampling point), resulting in two parallel samples at each sampling point.

To study the migration of heavy metals (arsenic (As), cadmium (Cd), chromium (Cr), copper (Cu), mercury (Hg), nickel (Ni), plumbum (Pb), zinc (Zn)) in HWI, the concentrations of heavy metals in raw material, fly ash, and bottom slag were determined through microwave digestion. In the process of digestion, 100 mg sample is fully digested in the solution of 12 ml HNO<sub>3</sub> + 8 ml HCl + 4 mL HF + 4 ml H<sub>2</sub>O in a microwave oven. Then, the digested solution is detected by the inductively coupled plasma, combined with mass spectrometry (Agilent 7700). Besides, the chlorinity (Cl) in fly ash and bottom slag is analyzed by X-ray Fluorescence Spectrometer (Shimadzu EDX 720).

The degree of chlorination (d<sub>c</sub>) of PCDD/F is computed as:

$$d_c = \sum_{i=4}^8 p_i \times n_i \quad (1)$$

Where p<sub>i</sub> is the weight percentage of Tri- to Oct- PCDD, PCDF, PCDD/F congeners, n<sub>i</sub> is the number of substituted chlorine atoms of PCDD/F congeners.

The migration rate (MR) of PCDD/F is calculated as:

$$MR(\%) = \frac{C_{in} - C_{out}}{C_{total}} \times 100\% \quad (2)$$

Where C<sub>in</sub> represents the concentrations (ng/Nm<sup>3</sup>) of PCDD, PCDF, PCDD/F, and the congeners at the inlet of every unit, and C<sub>out</sub> represents the concentrations (ng/Nm<sup>3</sup>) after every unit, C<sub>total</sub> represents the concentrations (ng/Nm<sup>3</sup>) at the outlet of the quench tower.

To assess the distribution characteristic of heavy metals in the residues including bottom slag and fly ash, the relative enrichment index (REI) (Li et al., 2018) is employed by the following equation:

$$REI = C_{i,ash} \frac{A_{ash,HW}}{C_{i,HW}} \quad (3)$$

Where C<sub>i,ash</sub> and C<sub>i,HW</sub> are the concentrations (mg/kg) of heavy metals in the residues after incineration and raw waste, respectively; A<sub>ash,HW</sub> is the ash content (wt%) in the air-dried waste raw material. Hence, REI can be used to describe the relative enrichment ratio of one type of heavy metal in fly ash (boiler ash, quench tower ash, and fabric filter ash) or bottom slag.

### 2.3. Statistical analysis

To describe 2,3,7,8-substituted congeners signatures during incineration, the signatures of the certain congeners are calculated based on their weight proportion (wt.%) within their own groups (OCDD or OCDF within PCDD or PCDF) (Chen et al., 2018). Moreover, Pearson correlation coefficients are used to quantize the relationship among PCDD/F, chlorinity, and heavy metals. Besides, the principal component analysis (PCA) method is utilized to investigate the relationship and differences

among PCDD/F, chlorinity, and heavy metals.

## 3. Results and discussion

### 3.1. Phase distribution of PCDD/F

Fig. 2. (a) (b) shows the total mass concentrations and I-TEQ in each sampling point. Overall, the APCD reduces total PCDD/F concentrations from 52.9 ng/Nm<sup>3</sup> to 3.26 ng/Nm<sup>3</sup> (0.697–0.0484 ng I-TEQ/Nm<sup>3</sup>). The PCDD/F I-TEQ after quench tower outlet is 0.697 ng I-TEQ/Nm<sup>3</sup>, which is higher than the legal limit of 0.5 ng I-TEQ/Nm<sup>3</sup> in China. It is clear that the mass concentrations and I-TEQ are declining in the order of A, B, C, D as the flue gas flows along with the APCD. The total PCDD/F concentrations are reduced by DS + ACI to 25.2 ng/Nm<sup>3</sup> (0.268 ng I-TEQ/Nm<sup>3</sup>). Then FF further decreases the total PCDD/F concentrations to 12.8 ng/Nm<sup>3</sup> (0.167 ng I-TEQ/Nm<sup>3</sup>). After the WS, the total PCDD/F concentrations are decreased to 3.26 ng/Nm<sup>3</sup> (0.0484 ng I-TEQ/Nm<sup>3</sup>). There is no memory effect observed, benefiting from the clean of APCD, consistent with the previous study (Zhong et al., 2020). Compared with the PCDD/F emission (0.72 ng I-TEQ ng/Nm<sup>3</sup>) (Wang et al., 2019) from HWI, the emission at stack is far small, even if below the national standard for municipal waste incineration (0.1 ng I-TEQ/Nm<sup>3</sup>). The ultra-low PCDD/F emission at the stack can be by reason of the high SO<sub>2</sub> concentration (3000 parts per million) before WS in Fig. S1. The reason will be discussed in section 3.4 in detail.

Apart from the PCDD/F emission levels, the phase distribution along with APCD is investigated. After ACI, the solid phase of PCDD/F concentration increases from 2.42 ng/Nm<sup>3</sup> to 10.1 ng/Nm<sup>3</sup> (0.047 I-TEQ ng/Nm<sup>3</sup> to 0.078 I-TEQ ng/Nm<sup>3</sup>), while the gas phase of PCDD/F concentration decreases from 50.5 ng/Nm<sup>3</sup> to 15.1 ng/Nm<sup>3</sup> (0.65 I-TEQ ng/Nm<sup>3</sup> to 0.19 I-TEQ ng/Nm<sup>3</sup>). The result indicates the gas phase of PCDD/F is adsorbed to be transformed into the solid phase by the ACI. Furthermore, the injection of NaHCO<sub>3</sub> can remove part of PCDD/F concentration according to the mass balance. Fig. 2(c)(d) shows the gas-/solid-phase fractions of PCDD/F mass concentrations at four sampling sites, along with I-TEQ. After the FF (sampling point C), the fraction of solid-phase PCDD/F concentration decreases to 11.4%, while the gas phase percentage comes back near that at sampling point A. The result indicates that the FF mainly removes the solid phase of PCDD/F. Furthermore, the fractions of gas-phase PCDD/F are much higher than those in solid-phase at all sampling points. The gas- and solid-phase distribution patterns are consistent at all sampling points.

### 3.2. Migration of PCDD/F congeners

#### 3.2.1. PCDD/F congeners distribution

PCDD/F congeners profiles have been employed to elucidate the formation mechanism (Cunliffe and Williams, 2009; Yang et al., 2017), and to identify the sources and migration behavior (Colombo et al., 2013). As shown in Fig. 3, the 2,3,7,8-substituted and 136 PCDD/F congeners are used to further analysis, including congeners concentrations and fingerprint. The 1,2,3,4,6,7,8-HpCDF dominates among 2,3,7,8-substituted congeners at all sampling points, which is different from OCDD in MSWI (Lin et al., 2020; Zhong et al., 2020). While, TCDF dominates among the 136 congeners, indicating that the chlorination reaction of PCDD/F is suppressed in the HWI. For solid-phase PCDD/F, OCDD is the congener with the highest concentration at the sampling point A, C (Table S1), and 1,2,3,4,7,8-HxCDD is dominated at the sampling point B. It is obvious that the proportion of PCDF is consistently lower than that of PCDD before WS. The result indicates that PCDD is easier adsorbed on the particulates than PCDF when the temperature is higher than 140 °C. However, 1,2,3,4,7,8-HxCDF is dominated at the sampling point D, due to the mainly PCDD released to the flue gas in the effect of WS at 140 °C.

For PCDD/F I-TEQ in Fig. S2/S3, 2,3,4,7,8-PeCDF takes approximately 25%–30% of total values at all sampling points, following by

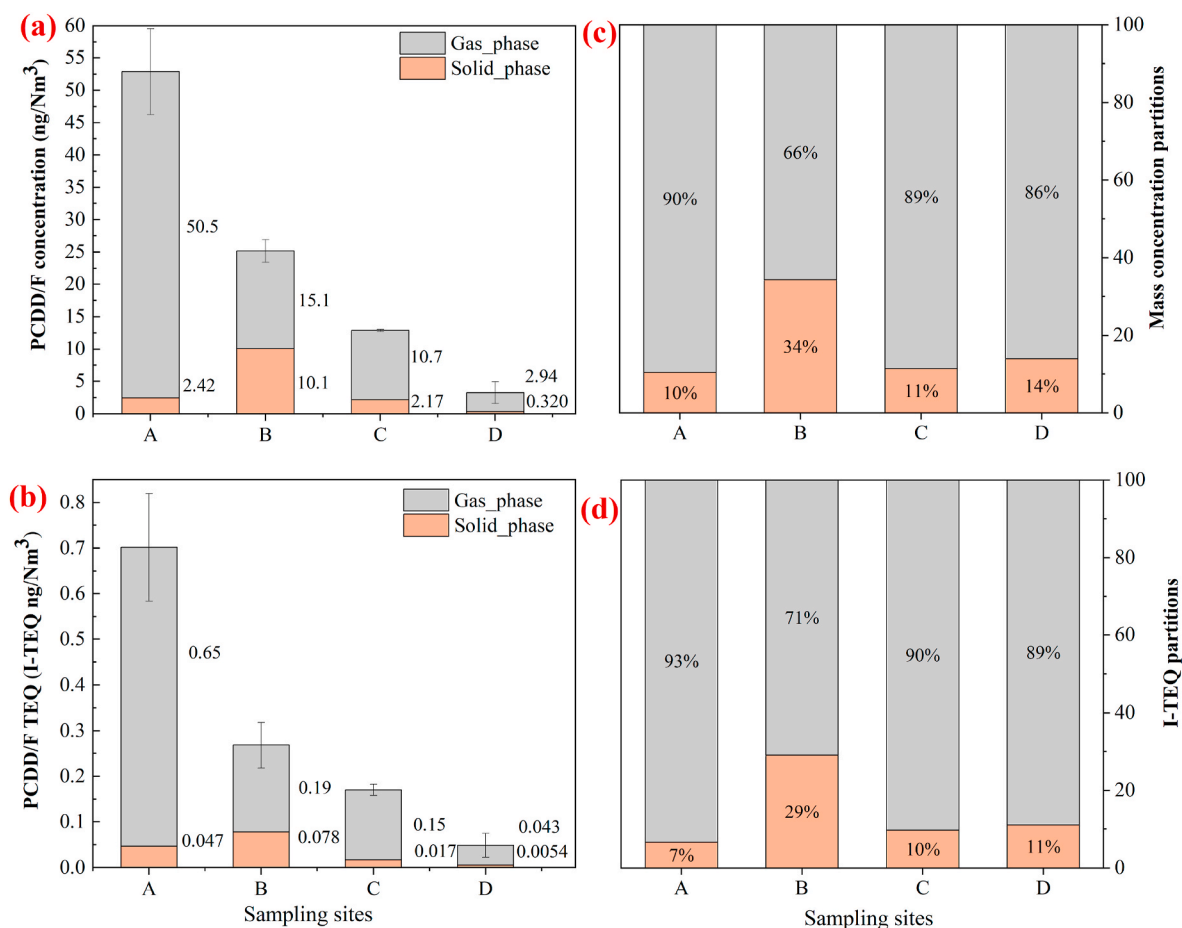


Fig. 2. (a) (b): PCDD/F mass concentrations and I-TEQ at four sampling points; (c) (d): phase distribution of PCDD/F mass concentrations and I-TEQ at four sampling points.

1,2,3,7,8-PeCDD, 1,2,3,4,7,8-HxCDF. And, the congener distribution patterns are mostly consistent among the sampling point A, C, D, excluding sampling point B. The contribution of 1,2,3,4,7,8-HxCDD is observed a distinct increase, while the contribution of 1,2,3,6,7,8-HxCDF significantly decreases at sampling point B. Meanwhile, as shown in Fig. 3(b), the 1,2,3,4,7,8-HxCDD concentration increases from 0.093 ng/Nm<sup>3</sup> to 0.04 ng/Nm<sup>3</sup>. The result indicates that 1,2,3,4,7,8-HxCDD is formed after the injection of AC and NaHCO<sub>3</sub>, and might be transformed by the congeners like 1,2,3,6,7,8-HxCDF. The abnormal change was observed in the previous study (Zhou et al., 2015).

The chlorination degree ( $d_c$ ) was calculated as Equation (1) to evaluate the impact of four APCD units on the chlorination reaction of PCDD/F. As shown in Fig. 4(b), the chlorination degree of PCDF is lower than that of PCDD at all sampling points, consistent with the study about municipal solid waste (Lin et al., 2020). The result indicates that PCDD is easier chlorinated than PCDF during incineration. The DS + ACI increases the PCDD/F chlorination degree from 4.82 to 5.16, because of the release of high chlorinated PCDD/F from the small particles (diameters from 0.1 to 1 mm) (Chi et al., 2005). Then, WS increases the PCDD/F chlorination degree from 4.99 to 5.30 due to the increasing of  $d_{c,PCDD}$ , suggesting that low chlorinated PCDD/F is preferred removed by WS.

As shown in Fig. 4(b), the ratio of PCDF to PCDD is higher than 1 at sampling point A, indicating that the PCDD/F formation in the study is dominant by de novo synthesis and chlorobenzene route synthesis. Besides, the PCDF/PCDD ratio (>1) at the sampling point A, D is higher than that (<1) in the HWI fed with a high level of phenolic waste (Wang et al., 2019). The reason is that the formation of PCDD is easier than that of PCDF in chlorophenol synthesis (Nganai et al., 2014). Furthermore,

for chlorophenol (CP) route synthesis, eight special congeners (Blaha and Hagenmaier, 1995; Sidhu et al., 1995; Zhang et al., 2017) are identified to calculate the relative importance of the CP route in Table S2. It is clear that the relative importance of the CP route synthesis hardly changes in four sampling points, ranging from 23.04% to 23.70%. Compared to the relative importance in previous study (Chen et al., 2018, 2019), the relative importance of CP route for HWI is higher than that for municipal solid waste incineration or co-combustion of municipal solid waste and coal.

### 3.2.2. Migration behavior of congeners

Table 2 shows the migration rate (%) of PCDD/F congeners along with APCD and Fig. 4 (a) shows the migration behavior of PCDD/F emissions along with APCD. For the migration of PCDD/F mass concentrations, 52.37% of PCDD/F is adsorbed by the AC&NaHCO<sub>3</sub>, exhibiting the greatest contribution. Moreover, 21.84% of PCDD/F is transferred to fly ash, followed by NaOH solution (15.38%). The vast (93.5%) PCDD/F migrates from the flue gas after quench tower to AC&NaHCO<sub>3</sub>, fly ash, and NaOH solution. Only 6.49% of PCDD/F emissions are emitted to the atmosphere.

For gas-phase and solid-phase PCDD/F, the migration rates to AC&NaHCO<sub>3</sub> are 70.1% and -315%, respectively. Then, MR<sub>fly ash</sub> of solid-phase (326%) is higher than that of gas-phase (8.69%). The result indicates that PCDD/F firstly migrates the solid phase (AC&NaHCO<sub>3</sub>), then is removed in the form of fly ash. Moreover, the MR of PCDF is higher than that of PCDD to AC&NaHCO<sub>3</sub> (52.2% vs 52.5%), fly ash (17.9% vs 26.1%). The MR<sub>AC&NaHCO3</sub> values exhibit the lowest peak value in PeCDD and HpCDF from TCDD/F to OCDD/F, like a concave curve. In general, for the PCDD/F absorbed by AC, MR<sub>AC</sub> values decrease

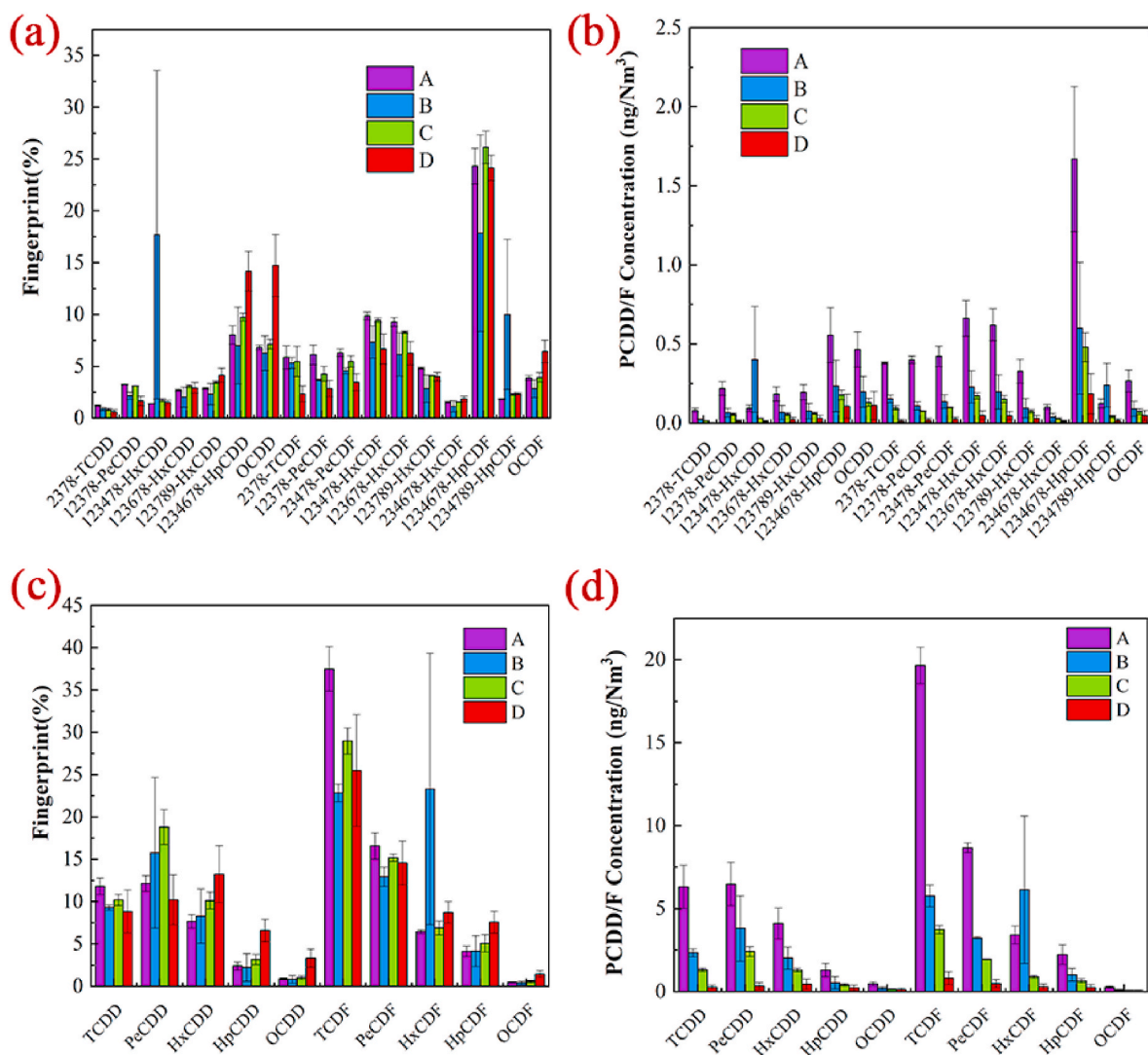


Fig. 3. (a) (b): Homologues 2,3,7,8-substituted congeners concentrations and fingerprint of PCDD/Fs in sampling points; (c) (d): Homologues 136 congeners concentrations and fingerprint of PCDD/Fs in sampling points.

with a decreasing chlorination degree of PCDD congeners or PCDF congeners due to the vapor pressure (Zhou et al., 2015). The abnormal reason can be the effect of  $\text{NaHCO}_3$  injection, and the temperature of FF above the optimal temperature ( $150\text{ }^\circ\text{C}$ ), resulting in the high chlorinated PCDD/F congeners ( $d_c > 5$ ) releasing from the small particles. As for 2,3,7,8-substituted congeners (Table S2), the  $\text{MR}_{\text{AC}}$  of 1,2,3,4,7,8-HxCDD, 1,2,3,4,7,8,9-HpCDD is  $-330\%$  and  $-94.0\%$ , respectively. The abnormal change could be affected by variations in gas/solid partition of congeners (Li et al., 2008).

For PCDD/F in gas-/solid-phase, MR values to NaOH solution, both show positive and excellent results. The MR of solid-phase PCDD/F is 85.2%, higher than that (72.5%) of gas-phase PCDD/F. Besides, the  $\text{MR}_{\text{NaOH}}$  values present a decreasing trend with the increasing chlorination degree of PCDD congeners or PCDF congeners. The result is opposed to the gas-phase PCDD/F migration with memory effect (Cunliffe and Williams, 2009), consistent with the  $\text{MR}_{\text{NaOH}}$  of solid-phase PCDD/F. The reason can be that the PCDD/F congeners are first absorbed into the particulates, then removed by the NaOH solution.

### 3.2.3. 2,3,7,8-Substituted congeners signatures

Among PCDD/F congeners, 2,3,7,8-substituted congeners are paid important attention due to the prominent toxicity. Furthermore, the precedence for chlorination on the 2,3,7,8-substituted congeners can

guide the investigation of evolution and mechanism, indicating the electrophilic aromatic substitution sequence. For the description of 2,3,7,8-substituted congeners, Hagenmaier profiles are presented in Table 3 by calculating the signal intensity of 2,3,7,8-substitutions among their own homologues groups.

As shown in Table 3, the average signal intensity for A, B, C, D sampling sites is 13.38%, 11.73%, 13.23%, 13.60%. The signal intensity of 2,3,7,8-substituted congeners is near equal in A, C sampling sites. The lowest signal intensity assembles after DS+ACI (the sampling point B), while the proportion of 1,2,3,4,7,8+1,2,3,6,7,8+1,2,3,7,8,9+2,3,4,6,7,8-HxCDF decreases from 50.11% to 9.07%, and 1,2,3,4,6,8-HpCDF decreases from 74.77% to 59.08%, respectively, though 1,2,3,4,7,8-HxCDD and 1,2,3,4,7,8,9-HpCDF increase from 2.27% to 19.80%, from 5.55% to 23.69%, respectively. The result indicates that the proportion of 2,3,7,8-substituted congeners declines in the effect DS+ACI. There is an obvious increase in the proportion of HpCDD, HpCDF, OCDD/F at the stack, indicating the increasing proportion of high chlorinated PCDD/F. The result is consistent with the analysis of the chlorination degree. Furthermore, the proportion of 2,3,7,8-substituted congeners increases from 13.23% before WS to 13.60% after WS. The result indicates that the PCDD/F congeners except 2,3,7,8-substituted congeners are easier removed by WS than 2,3,7,8-substituted congeners. Furthermore, for the chlorination of DD/DF,

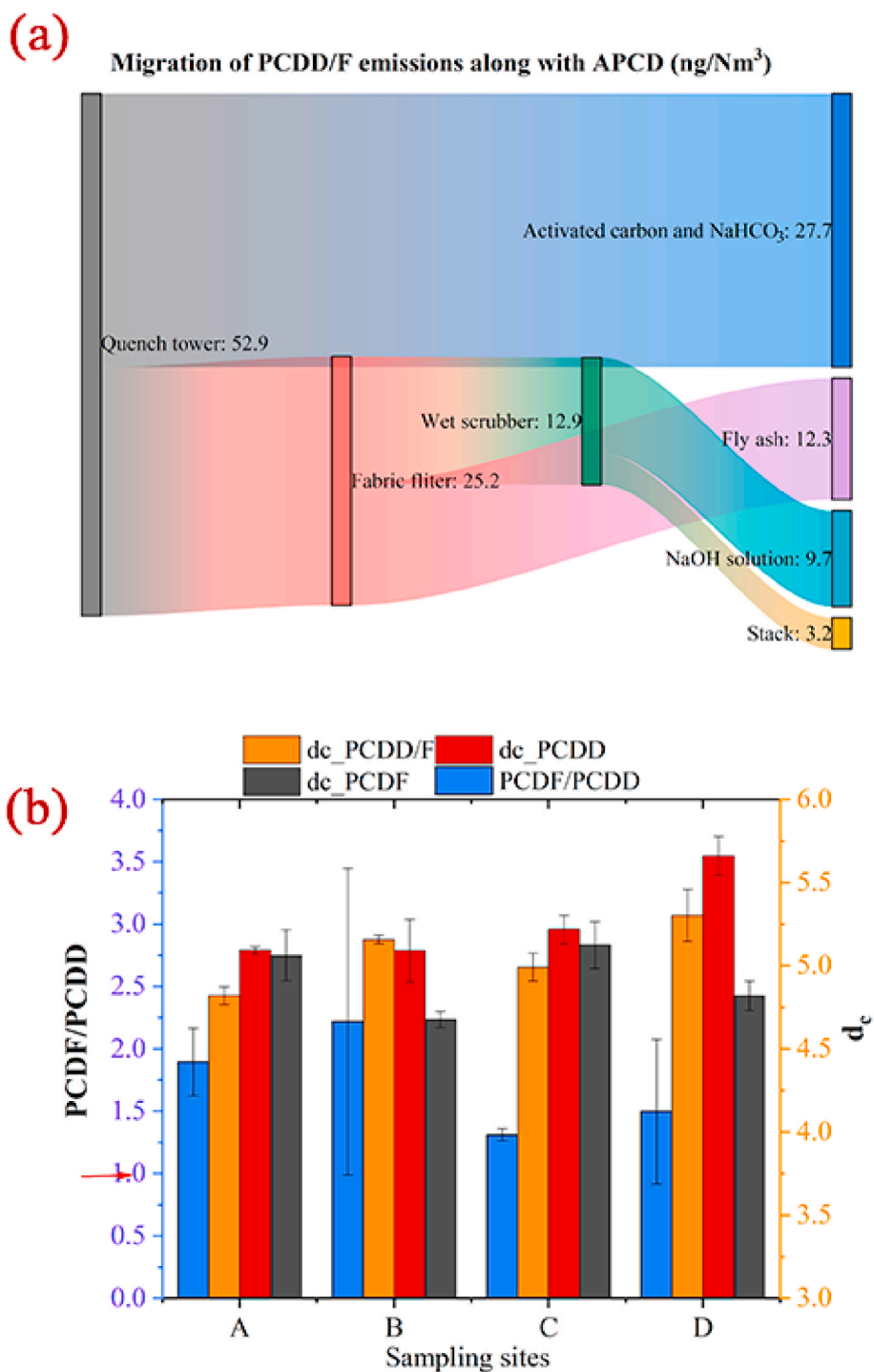


Fig. 4. (a): Migration of PCDD/F emissions along with APCD; (b): the degrees of chlorination ( $d_c$ ) of PCDD/F, PCDD, PCDF, and ratios of PCDF to PCDD.

Hagenmaier Profile can be utilized to present the average signal intensity. Compared to the average signal intensity in the previous studies (Chen et al., 2018, 2019), the average signal intensity of DD/DF chlorination for HWI is higher than that for municipal solid waste incineration or co-combustion of municipal solid waste and coal.

### 3.3. Heavy metals distribution characteristic and migration behavior

According to the mass balance, previous studies have shown that heavy metals in the flue gas account for a relatively small proportion (<10%) (Li et al., 2018). Therefore, the study mainly concerns the

emission characteristics and migration behavior of heavy metals in bottom slag and fly ash.

#### 3.3.1. Distribution characteristic

According to the National Hazardous Waste Catalogue in China, the residues (including bottom slag, boiler ash, quench tower ash, and fabric filter ash) from HWI are identified as HW18, because of the enrichment of PCDD/F and heavy metals. Table 4 shows the concentrations of heavy metals and chlorinity in raw waste and solid residues.

In the work, the yields of bottom slag, fly ash (boiler ash, quench tower ash, and bag filter ash) are averagely 15.5 t/d, 9.7 t/d,

**Table 2**  
Migration rate (%) of PCDD/F congeners along with APCD.

Migration rate (%)	AC&NaHCO <sub>3</sub>	Fly ash	NaOH solution	Stack	Sum
TeCDD	62.84	16.34	16.62	4.20	100
PeCDD	41.17	21.43	32.24	5.16	100
HxCDD	50.61	17.72	20.80	10.87	100
HpCDD	59.14	9.51	13.95	17.40	100
OCDD	57.42	14.39	4.26	23.93	100
PCDD	52.23	17.89	22.47	7.41	100
TeCDF	70.65	10.35	14.91	4.08	100
PeCDF	62.65	14.78	17.02	5.55	100
HxCDF	-79.86	153.94	17.39	8.54	100
HpCDF	54.54	16.31	17.64	11.51	100
OCDF	66.01	6.66	9.61	17.72	100
PCDF	52.53	26.16	15.83	5.49	100
PCDD/F	52.37	21.84	19.29	6.49	100
Gas PCDD/F	70.10	8.69	15.38	5.83	100
Solid PCDD/F	-315.90	326.31	76.38	13.21	100

**Table 3**  
Hagenmaier Profile of PCDD/F in four APCD points.

Hagenmaier profile (%)	A	B	C	D
2378-TCDD	1.28	1.04	1.11	1.48
12378-PeCDD	3.38	1.74	2.33	3.64
123478-HxCDD	2.27	19.80	2.37	2.40
123678-HxCDD	4.48	3.29	4.33	4.87
123789-HxCDD	4.76	3.75	4.80	6.84
1234678-HpCDD	42.74	44.19	43.75	47.08
OCDD	2.49	2.22	2.35	8.04
2378-TCDF	1.93	2.66	2.57	1.96
12378-PeCDF	4.61	3.36	3.89	4.23
23478-PeCDF	4.86	4.23	5.03	5.19
123478-HxCDF	19.37	3.72	19.38	16.95
123678-HxCDF	18.17	3.21	17.07	15.98
123789-HxCDF	9.59	1.53	8.43	10.23
234678-HxCDF	2.98	0.61	3.23	4.36
1234678-HpCDF	74.77	59.08	73.73	72.06
1234789-HpCDF	5.55	23.69	6.46	6.70
OCDF	0.78	0.56	1.00	2.51
Average <sup>a</sup>	13.38	11.73	13.23	13.60

<sup>a</sup> Average signal intensity of 2,3,7,8-substitutions expect for OCDD and OCDF.

respectively. In the raw material, the heavy metals with the highest concentration is Zn (1585.98 mg/kg), resulting in the highest concentration (12855.41 mg/kg) in boiler ash, in the form of zinc chloride over the temperature range (500 °C–1000 °C). And the Hg presents the lowest concentration (0.74 mg/kg), similar to Cd (1.96 mg/kg). As for Cu, the concentration in raw materials is 101.46 mg/kg, while the concentration in the bottom slag is 1475.41 mg/kg. The result indicates that Cu enriches in the bottom slag due to Cu being inclined to deposit into flue gas as CuSO<sub>4</sub> (Lu et al., 2021) rather than the volatile substance as Cu<sub>3</sub>Cl<sub>3</sub> and CuCl (Chen et al., 1998) in the condition of the SO<sub>2</sub> concentrations being as high as 3000 parts per million. Compared with the previous study in HWI, the heavy metals concentrations are higher than those in (Wang et al., 2020) except Ni and Hg, lower than those in (Li et al., 2018) except Cr. The result indicates that the heavy metals concentrations are determined by the composition of HW. Besides, the concentrations of heavy metals are far higher than those from sludge-coal co-combustion (Zhang et al., 2008, 2013). The distribution

**Table 4**  
Emission and distribution characteristic of heavy metals and chlorinity.

Unit (mg/kg)	As	Cd	Cr	Cu	Hg	Ni	Pb	Zn	Cl
Hazardous material	14.38	1.96	340.32	101.46	0.74	32.82	382.97	1585.98	5.26
Bottom slag	63.00	0.60	435.37	1475.41	0.89	613.21	43.24	801.06	1.55
Boiler ash	52.13	1.62	326.08	910.59	2.16	58.28	7108.82	12855.41	5.40
Quench tower ash	5.23	0.59	86.66	159.18	2.35	8.00	1243.87	1705.81	30.16
Farbic filter ash	8.82	0.64	106.61	203.74	1.79	5.84	1822.15	1704.58	30.97

characteristics of heavy metals along with APCD favor the detection and capture of heavy metals (Awual, 2019b, c; Awual and Hasan, 2015, 2019; Awual et al., 2019; Islam, A. et al., 2019a).

### 3.3.2. Migration behavior

To elaborate on the distribution pattern and migration of heavy metals in HWI, the relative enrichment indexes (REI) are computed through equation (3). The REI of heavy metals in bottom slag and fly ash is shown in Fig. 5(a). Obvious enrichments of Pb, Zn, Hg, Cd were observed in fly ash. Compared with the previous study in HWI (Li et al., 2018; Wang et al., 2020), the distribution pattern of heavy metals (Pb, Zn, Hg, Cd) is consistent. The result indicates that the migration behavior of the above volatile heavy metals is consistent (Chen et al., 1999). Besides, the REI of Cu, As, Cr in fly ash is near to that in the bottom slag, considered as the medium-volatiles heavy metals in the HWI. The result indicates that half of Cu, As and Cr tend to form non-volatile matter. Moreover, the REI in the bottom slag is far higher than that in fly ash for Ni. Hence, the source of Ni in fly ash is mainly from the entrainment in the process of migration.

Fig. 6 present the mass distribution proportion of the heavy metals, and Fig. S4 shows the concentrations and distribution pattern of heavy metals in raw material, bottom slag, and fly ash. More than 46% As, Cr, Cu enrich in the bottom slag (>1000 °C), indicating the low vapor pressure. In addition, more than 70% Pb and Zn enrich in the boiler ash (500–1000 °C), reflecting high vapor pressure. Except for, all the heavy metals concentrations in the quench tower ash are lower than those in boiler ash and fabric filter ash. In detail, the concentrations of heavy metals excluding Hg in boiler ash are as high as ten times that in quench tower ash. The result indicates that the heavy metals concentrations are closely correlated with the residence time except for the high volatile metals like Hg, which is mainly in the gas phase. Therefore, the migration behavior of heavy metals in the incinerator is dependent on the evaporative properties and residence time.

### 3.4. Relationship between heavy metals and PCDD/F

To investigate the relationship among PCDD/F I-TEQ, heavy metals, and chlorine content, PCA and Pearson correlation coefficients are introduced to analyze the correlation. As shown in Fig. 5(b), the sum of the two first factors reaches 97.04%, suggesting that the two factors can be to represent most of the information in the nine original variables. Factor 1 mainly retains the information of elements including As, Cr, Cu, Ni, Hg, and Cl, and the variance contribution rate is 55.37%. Besides, factor 2 mainly retains the information of elements including Pb, Cd, Zn, I-TEQ, and the variance contribution rate is 42.04%. According to the theory of factor analysis, the correlation between two variables can be judged by the angle between two variables in the factor loading diagram. It can be found that As, Cr, Cu are concentrated in the first quadrant and located closely. As has a positive coefficient of 0.993, 0.975 with Cr, Cu, respectively, with a negative coefficient of -0.996 with Cl (Table 5). The results indicate that the distribution pattern and migration of As are consistent with Cr, Cu. Moreover, Pb, Cd, Zn are concentrated in the positive semi-axis of factor 2 and located closely. Pb has a positive coefficient of 0.977, 0.985 with Cd, Zn, respectively. However, Hg as a volatile heavy metal, like Pb, has a coefficient of 0.528 with Pb, resulting in a weak correlation. The reason can be that the Hg is

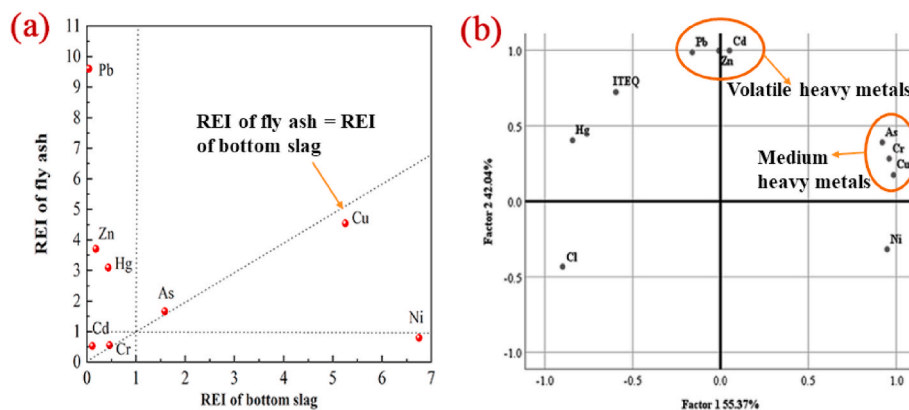


Fig. 5. (a) Partition characteristics of heavy metals in hazardous waste incineration; (b) Relationship among the heavy metals, chlorinity, and PCDD/F I-TEQ.

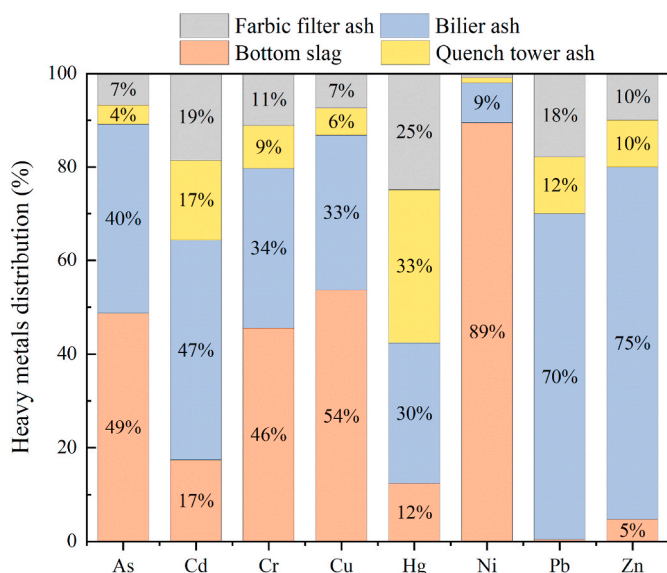


Fig. 6. Mass distribution proportion of the heavy metals.

main in the flue gas and removed by WS. The correlation coefficient between Hg and Ni is  $-0.924$ , indicating a strong negative correlation.

As shown in Table 5, I-TEQ has a highest correlation coefficient with Pb (0.815), following Ni ( $-0.798$ ), Zn (0.706), Cd (0.683), Hg (0.671), Cu ( $-0.464$ ), Cr ( $-0.366$ ), As ( $-0.267$ ), Cl (0.249). The results indicate that the PCDD/F formation is positively correlated with the volatile heavy metals (Pb, Zn, Cd, Hg) enriching in the boiler ash. The reason with a strong positive correlation can be that the reaction temperature for the precursor synthesis is located in the temperature range of the boiler (500–1000 °C). Furthermore, medium volatile heavy metals (Cu, Cr, As) have a weak and negative correlation with the formation of

PCDD/F. However,  $\text{CuCl}_2$  has been proven as the fastest catalytic rate catalyst for PCDD/F formation (Ryu et al., 2005). The Cl content is as low as 5.40% in the boiler ash and is 30.16% in the quench tower ash (Table 4). The results indicate that  $\text{CuCl}_2$  is mainly formed in/after the quench tower ( $>200$  °C) and a small portion of  $\text{CuCl}_2$  is present in the boiler ash. In addition, the  $\text{SO}_2$  had been proven to inhibit the formation of PCDD/F by converting  $\text{CuCl}_2$  to  $\text{CuSO}_4$ . Therefore, the inhibiting effect of  $\text{SO}_2$  with high concentrations for the PCDD/F formation is significant. The raw hazardous waste with high sulfur content can prevent the PCDD/F formation and the release of heavy metals into the atmosphere.

#### 4. Conclusion

To investigate the phase distribution, migration, and relationship of PCDD/F and heavy metals, a comprehensive investigation was conducted in a large-scale hazardous waste incinerator. The results are following:

- (1) The PCDD/F emissions are reduced by DS+ACI+FF+WS from  $52.9 \text{ ng/Nm}^3$  to  $3.26 \text{ ng/Nm}^3$  ( $0.697\text{--}0.0484 \text{ ng I-TEQ/Nm}^3$ ). High sulfur content in hazardous waste results in low PCDD/F and heavy metals emissions. TCDF isomers dominate the PCDD/F congeners, while 1,2,3,4,6,7,8-HpCDF dominates among 2,3,7,8-substituted congeners.
- (2) Due to high levels of chlorinity and heavy metals, the chlorophenol route synthesis and chlorination of DD/DF enhance. Based on the ratio of PCDF/PCDD, de novo synthesis and chlorobenzene synthesis are dominated formation pathways of PCDD/F.
- (3) The migration rate of PCDD/F to sodium bicarbonate and activated carbon is 52.4%, followed by fly ash (21.8%), sodium hydroxide solution (19.3%), atmosphere (6.5%). WS after clean-up is effective to remove PCDD/F emissions, especially solid-phase PCDD/F.

Table 5  
Pearson coefficients among heavy metals, chlorinity, and PCDD/F I-TEQ in the residues.

Coefficients	As	Cd	Cr	Cu	Hg	Ni	Pb	Zn	Cl
Cd	0.437								
Cr	0.993 <sup>b</sup>	0.331							
Cu	0.975 <sup>a</sup>	0.224	0.994 <sup>c</sup>						
Hg	$-0.617$	0.37	$-0.695$	$-0.755$					
Ni	0.749	$-0.268$	0.82	0.878	$-0.924$				
Pb	0.238	0.977 <sup>a</sup>	0.125	0.014	0.528	$-0.465$			
Zn	0.38	0.997 <sup>c</sup>	0.272	0.164	0.436	$-0.326$	0.985 <sup>b</sup>		
Cl	$-0.996c$	$-0.479$	$-0.984b$	$-0.961b$	0.555	$-0.716$	$-0.282$	$-0.427$	
I-TEQ	$-0.267$	0.683	$-0.366$	$-0.464$	0.671	$-0.798$	0.815	0.706	0.249

Note: a means  $p\text{-value} \leq 0.05$ ; b means  $0.05 < p\text{ value} \leq 0.01$ ; c means  $p\text{ value} < 0.005$ ; no marks means  $p\text{-value} > 0.1$ .

- (4) The migration behavior of heavy metals is dependent on the volatility properties of these metals. Cu is inclined to deposit into flue gas as  $\text{CuSO}_4$  rather than the volatile substance due to high levels of  $\text{SO}_2$ .
- (5) Statistically, PCDD/F emissions have the highest correlation coefficient with Pb (0.815), followed by Ni (-0.798). The PCDD/F formation is promoted by the volatile heavy metal (Pb, Zn, Cd, Hg), prevented by medium volatile heavy metals (Cu, Cr, As).

The study reveals the dominated formation mechanism, phase distribution of PCDD/F and heavy metals, and the relationship between heavy metals and PCDD/F. The results benefit to reducing the PCDD/F and heavy metals emissions from large-scale HWI, guiding the design and operation of APCD. In the future, the PCDD/F and heavy metals emissions will be investigated in different operating conditions to obtain optimal operating conditions.

#### CRedit authorship contribution statement

**Shijian Xiong:** Conceptualization, Methodology, Software, Data curation, Writing – original draft. **Yaqi Peng:** Writing-Reviewing, Investigation. **Ken Chen:** Formal analysis. **Shengyong Lu:** Writing-Reviewing, Supervision. **Wenqian Jiang:** Formal analysis. **Xiaodong Li:** Supervision. **Fei Wang:** Resources, Supervision. **Kefa Cen:** Supervision.

#### Declaration of competing interest

The authors declare that they have no known competing financial interests or personal relationships that could have appeared to influence the work reported in this paper.

#### Acknowledgment

This research is supported by the National Key Research and Development Program of China (2019YFC1907003).

#### Appendix A. Supplementary data

Supplementary data to this article can be found online at <https://doi.org/10.1016/j.jclepro.2022.130764>.

#### References

- Alam, M.M., Asiri, A.M., Uddin, M.T., Inamuddin, I., Islam, M.A., Awual, M.R., Rahman, M.M., 2019a. One-step wet-chemical synthesis of ternary  $\text{ZnO/CuO/Co}_3\text{O}_4$  nanoparticles for sensitive and selective melamine sensor development. *New J. Chem.* 43 (12), 4849–4858.
- Alam, M.M., Asiri, A.M., Uddin, M.T., Islam, M.A., Awual, M.R., Rahman, M.M., 2019b. Detection of uric acid based on doped  $\text{ZnO/Ag}_2\text{O/Co}_3\text{O}_4$  nanoparticle loaded glassy carbon electrode. *New J. Chem.* 43 (22), 8651–8659.
- Altwickler, E.R., 1996. Formation of PCDD/F in municipal solid waste incinerators: laboratory and modeling studies. *J. Hazard Mater.* 47 (1), 137–161.
- Awual, M.R., 2015. A novel facial composite adsorbent for enhanced copper(II) detection and removal from wastewater. *Chem. Eng. J.* 266, 368–375.
- Awual, M.R., 2017. Novel nanocomposite materials for efficient and selective mercury ions capturing from wastewater. *Chem. Eng. J.* 307, 456–465.
- Awual, M.R., 2019a. An efficient composite material for selective lead(II) monitoring and removal from wastewater. *J. Environ. Chem. Eng.* 7 (3).
- Awual, M.R., 2019b. Efficient phosphate removal from water for controlling eutrophication using novel composite adsorbent. *J. Clean. Prod.* 228, 1311–1319.
- Awual, M.R., 2019c. Mesoporous composite material for efficient lead(II) detection and removal from aqueous media. *J. Environ. Chem. Eng.* 7 (3).
- Awual, M.R., Hasan, M.M., 2015. Fine-tuning mesoporous adsorbent for simultaneous ultra-trace palladium(II) detection, separation and recovery. *J. Ind. Eng. Chem.* 21, 507–515.
- Awual, M.R., Hasan, M.M., 2019. A ligand based innovative composite material for selective lead(II) capturing from wastewater. *J. Mol. Liq.* 294.
- Awual, M.R., Hasan, M.M., Asiri, A.M., Rahman, M.M., 2019. Cleaning the arsenic(V) contaminated water for safe-guarding the public health using novel composite material. *Composites Part B* 171, 294–301.

- Belevi, H., Moench, H., 2000. Factors determining the element behavior in municipal solid waste incinerators. 1. Field studies. *Environ. Sci. Technol.* 34 (12), 2501–2506.
- Bhavsar, S.P., Reiner, E.J., Hayton, A., Fletcher, R., MacPherson, K., 2008. Converting Toxic Equivalents (TEQ) of dioxins and dioxin-like compounds in fish from one Toxic Equivalency Factor (TEF) scheme to another. *Environ. Int.* 34 (7), 915–921.
- Blaha, J., Hagenmaier, H., 1995. Time dependence of the de novo synthesis of PCDD/PCDF and potential precursors on a model fly ash. *Organohalogen Compd.* 23 (403), e406.
- Cao, X., Ji, L., Lin, X., Stevens, W.R., Tang, M., Shang, F., Tang, S., Lu, S., 2018. Comprehensive diagnosis of PCDD/F emission from three hazardous waste incinerators. *R. Soc. Open Sci.* 5 (7), 172056.
- Chang, M.B., Huang, C.K., Wu, H.T., Lin, J.J., Chang, S.H., 2000. Characteristics of heavy metals on particles with different sizes from municipal solid waste incineration. *J. Hazard Mater.* 79 (3), 229–239.
- Chen, J.-C., Wey, M.-Y., Ou, W.-Y., 1999. Capture of heavy metals by sorbents in incineration flue gas. *Sci. Total Environ.* 228 (1), 67–77.
- Chen, J.-C., Wey, M.-Y., Su, J.-L., Hsieh, S.-M., 1998. Two-stage simulation of the major heavy-metal species under various incineration conditions. *Environ. Int.* 24 (4), 451–466.
- Chen, T., Sun, C., Wang, T., Zhan, M., Li, X., Lu, S., Yan, J., 2020. Removal of PCDD/Fs and CBzs by different air pollution control devices in MSWIs. *Aerosol Air Qual. Res.* 20 (10), 2260–2272.
- Chen, Z., Lin, X., Lu, S., Li, X., Qiu, Q., Wu, A., Ding, J., Yan, J., 2018. Formation pathways of PCDD/Fs during the Co-combustion of municipal solid waste and coal. *Chemosphere* 208, 862–870.
- Chen, Z., Mao, Q., Lu, S., Buekens, A., Xu, S., Wang, X., Yan, J., 2017. Dioxins degradation and reformation during mechanochemical treatment. *Chemosphere* 180, 130–140.
- Chen, Z.L., Lin, X.Q., Lu, S.Y., Li, X.D., Yan, J.H., 2019. Suppressing formation pathway of PCDD/Fs by S-N-containing compound in full-scale municipal solid waste incinerators. *Chem. Eng. J.* 359, 1391–1399.
- Chi, K.H., Chang, M.B., Chang-Chien, G.P., Lin, C., 2005. Characteristics of PCDD/F congener distributions in gas/particulate phases and emissions from two municipal solid waste incinerators in Taiwan. *Sci. Total Environ.* 347 (1), 148–162.
- Colombo, A., Benfenati, E., Bugatti, S.G., Lodi, M., Mariani, A., Musmeci, L., Rotella, G., Senese, V., Ziemacki, G., Fanelli, R., 2013. PCDD/Fs and PCBs in ambient air in a highly industrialized city in Northern Italy. *Chemosphere* 90 (9), 2352–2357.
- Cunliffe, A.M., Williams, P.T., 2009. De-novo formation of dioxins and furans and the memory effect in waste incineration flue gases. *Waste Manag.* 29 (2), 739–748.
- Evans, J., Williams, P.T., 2000. Heavy metal adsorption onto flyash in waste incineration flue gases. *Process Saf. Environ. Protect.* 78 (1), 40–46.
- Gullett, B.K., Touati, A., Lee, C.W., 2000. Formation of chlorinated dioxins and furans in a hazardous-waste-firing industrial boiler. *Environ. Sci. Technol.* 34 (11), 2069–2074.
- Huang, H., Buekens, A., 1996. De novo synthesis of polychlorinated dibenzo-p-dioxins and dibenzofurans Proposal of a mechanistic scheme. *Sci. Total Environ.* 193 (2), 121–141.
- Islam, A., Teo, S.H., Awual, M.R., Taufiq-Yap, Y.H., 2019a. Improving the hydrogen production from water over MgO promoted Ni-Si/CNTs photocatalyst. *J. Clean. Prod.* 238.
- Islam, M.A., Awual, M.R., Angove, M.J., 2019b. A review on nickel(II) adsorption in single and binary component systems and future path. *J. Environ. Chem. Eng.* 7 (5).
- Kamel, R.M., Shahat, A., Hegazy, W.H., Khodier, E.M., Awual, M.R., 2019. Efficient toxic nitrite monitoring and removal from aqueous media with ligand based conjugate materials. *J. Mol. Liq.* 285, 20–26.
- Ke, S., Jianhua, Y., Xiaodong, L., Shengyong, L., Yinglei, W., Muxing, F., 2010. Inhibition of de novo synthesis of PCDD/Fs by  $\text{SO}_2$  in a model system. *Chemosphere* 78 (10), 1230–1235.
- Kubra, K.T., Salman, M.S., Hasan, M.N., Islam, A., Hasan, M.M., Awual, M.R., 2021. Utilizing an alternative composite material for effective copper(II) ion capturing from wastewater. *J. Mol. Liq.* 336.
- Li, H.-W., Lee, W.-J., Tsai, P.-J., Mou, J.-L., Chang-Chien, G.-P., Yang, K.-T., 2008. A novel method to enhance polychlorinated dibenzo-p-dioxins and dibenzofurans removal by adding bio-solution in EAF dust treatment plant. *J. Hazard Mater.* 150 (1), 83–91.
- Li, M., Wang, C., Cen, K., Ni, M., Li, X., 2017. PCDD/F emissions during startup and shutdown of a hazardous waste incinerator. *Chemosphere* 181, 645–654.
- Li, W., Ma, Z., Huang, Q., Jiang, X., 2018. Distribution and leaching characteristics of heavy metals in a hazardous waste incinerator. *Fuel* 233, 427–441.
- Lin, X., Ma, Y., Chen, Z., Li, X., Lu, S., Yan, J., 2020. Effect of different air pollution control devices on the gas/solid-phase distribution of PCDD/F in a full-scale municipal solid waste incinerator. *Environ. Pollut.* 265 (Pt B), 114888.
- Lothgren, C.J., van Bavel, B., 2005. Dioxin emissions after installation of a polishing wet scrubber in a hazardous waste incineration facility. *Chemosphere* 61 (3), 405–412.
- Lou, R., Ahonkhai, S.I., 2002. Radical/radical vs radical/molecule reactions in the formation of PCDD/Fs from (chloro)phenols in incinerators. *Chemosphere* 46 (9), 1273–1278.
- Lu, S., Xiang, Y., Chen, Z., Chen, T., Lin, X., Zhang, W., Li, X., Yan, J., 2021. Development of phosphorus-based inhibitors for PCDD/Fs suppression. *Waste Manag.* 119, 82–90.
- Margallo, M., Taddei, M.B.M., Hernández-Pellón, A., Aldaco, R., Irabien, A., 2015. Environmental sustainability assessment of the management of municipal solid waste incineration residues: a review of the current situation. *Clean Technol. Environ. Policy* 17 (5), 1333–1353.
- National Bureau of Statistics of China. *China Statistical Yearbook*.
- Nganai, S., Dellinger, B., Lomnicki, S., 2014. PCDD/PCDF ratio in the precursor formation model over CuO surface. *Environ. Sci. Technol.* 48 (23), 13864–13870.

- Rahman, M.M., Hussain, M.M., Arshad, M.N., Awual, M.R., Asiri, A.M., 2019. Arsenic sensor development based on modification with (E)-N'-(2-nitrobenzylidene)-benzenesulfonohydrazide: a real sample analysis. *New J. Chem.* 43 (23), 9066–9075.
- Ruokojärvi, P., Asikainen, A., Ruuskanen, J., Tuppurainen, K., Kilpinen, C.M., Pia Yli-Keturi, N., 2001. Urea as a PCDD/F inhibitor in municipal waste incineration. *J. Air Waste Manag. Assoc.* 51 (3), 422–431.
- Ryan, S.P., Li, X.-d., Gullett, B.K., Lee, C.W., Clayton, M., Touati, A., 2006. Experimental study on the effect of SO<sub>2</sub> on PCDD/F emissions: determination of the importance of gas-phase versus solid-phase reactions in PCDD/F formation. *Environ. Sci. Technol.* 40 (22), 7040–7047.
- Ryu, J.-Y., Mulholland, J.A., Takeuchi, M., Kim, D.-H., Hatanaka, T., 2005. CuCl<sub>2</sub>-catalyzed PCDD/F formation and congener patterns from phenols. *Chemosphere* 61 (9), 1312–1326.
- Sheikh, T.A., Arshad, M.N., Rahman, M.M., Asiri, A.M., Marwani, H.M., Awual, M.R., Bawazir, W.A., 2017. Trace electrochemical detection of Ni<sup>2+</sup> ions with bidentate N, N'-(ethane-1,2-diyl)bis(3,4-dimethoxybenzenesulfonamide) [EDBDMBS] as a chelating agent. *Inorg. Chim. Acta.* 464, 157–166.
- Sheikh, T.A., Rahman, M.M., Asiri, A.M., Marwani, H.M., Awual, M.R., 2018. 4-Hexylresorcinol sensor development based on wet-chemically prepared Co<sub>3</sub>O<sub>4</sub>@Er<sub>2</sub>O<sub>3</sub> nanorods: a practical approach. *J. Ind. Eng. Chem.* 66, 446–455.
- Sidhu, S.S., Maqsood, L., Dellinger, B., Mascolo, G., 1995. The homogeneous, gas-phase formation of chlorinated and brominated dibenzo-p-dioxin from 2,4,6-trichloro- and 2,4,6-tribromophenols. *Combust. Flame* 100 (1), 11–20.
- Wang, C., Shao, N., Xu, J., Zhang, Z., Cai, Z., 2020. Pollution emission characteristics, distribution of heavy metals, and particle morphologies in a hazardous waste incinerator processing phenolic waste. *J. Hazard Mater.* 388, 121751.
- Wang, C., Xu, J., Yang, Z., Zhang, Z., Cai, Z., 2019. A field study of polychlorinated dibenzo-p-dioxins and dibenzofurans formation mechanism in a hazardous waste incinerator: emission reduction strategies. *J. Clean. Prod.* 232, 1018–1027.
- Xiong, S., Lu, S., Shang, F., Li, X., Yan, J., Cen, K., 2021. Online predicting PCDD/F emission by formation pathway identification clustering and Box-Cox Transformation. *Chemosphere* 274, 129780.
- Yan, J.H., Chen, T., Li, X.D., Zhang, J., Lu, S.Y., Ni, M.J., Cen, K.F., 2006. Evaluation of PCDD/Fs emission from fluidized bed incinerators co-firing MSW with coal in China. *J. Hazard Mater.* 135 (1), 47–51.
- Yang, L., Liu, G., Zheng, M., Zhao, Y., Jin, R., Wu, X., Xu, Y., 2017. Molecular mechanism of dioxin formation from chlorophenol based on electron paramagnetic resonance spectroscopy. *Environ. Sci. Technol.* 51 (9), 4999–5007.
- Zhang, G., Hai, J., Ren, M., Zhang, S., Cheng, J., Yang, Z., 2013. Emission, mass balance, and distribution characteristics of PCDD/Fs and heavy metals during cocombustion of sewage sludge and coal in power plants. *Environ. Sci. Technol.* 47 (4), 2123–2130.
- Zhang, H., He, P.J., Shao, L.M., 2008. Fate of heavy metals during municipal solid waste incineration in Shanghai. *J. Hazard Mater.* 156 (1–3), 365–373.
- Zhang, M., Buekens, A., Olie, K., Li, X., 2017. PCDD/F-isomers signature - effect of metal chlorides and oxides. *Chemosphere* 184, 559–568.
- Zhao, L., Li, C., Zhang, X., Zeng, G., Zhang, J., Xie, Y.e., 2015. A review on oxidation of elemental mercury from coal-fired flue gas with selective catalytic reduction catalysts. *Catal. Sci. Technol.* 5 (7), 3459–3472.
- Zhong, R., Wang, C., Zhang, Z., Liu, Q., Cai, Z., 2020. PCDD/F levels and phase distributions in a full-scale municipal solid waste incinerator with co-incinerating sewage sludge. *Waste Manag.* 106, 110–119.
- Zhou, X.J., Li, X.D., Ni, M.J., Cen, K.F., 2015. Removal efficiencies for 136 tetra- through octa-chlorinated dibenzo-p-dioxins and dibenzofuran congeners with activated carbons. *Environ. Sci. Pollut. Res. Int.* 22 (22), 17691–17696.